Science Bulletin 71 (2026) 538–546

Contents lists available at ScienceDirect

Science Bulletin

journal homepage: www.elsevier.com/locate/scib

Article

A fast powerful X-ray transient from possible tidal disruption of a white dwarf

Dongyue Li[a,1], Wenda Zhang[a,1,*], Jun Yang[b,1], Jin-Hong Chen[c,d,e,1], Weimin Yuan[a,f,*], Huaqing Cheng[a], Fan Xu[g], Xinwen Shu[g], Rong-Feng Shen[h,i], Ning Jiang[j], Jiazheng Zhu[j], Chang Zhou[k], Weihua Lei[k], Hui Sun[a], Chichuan Jin[a,f,l,*], Lixin Dai[c,d,*], Bing Zhang[c,d], Yu-Han Yang[m], Wenjie Zhang[a], Hua Feng[n], Bifang Liu[a,f], Hongyan Zhou[j,o], Haiwu Pan[a], Mingjun Liu[a], Stéphane Corbel[p], Sitha K. Jagan[q], Maria Cristina Baglio[r], Christopher R. Burns[s], Floriane Cangemi[t], Chun Chen[h,i,u], Yehao Cheng[v], Alexis Coleiro[t], Francesco Coti Zelati[w,x], Sourya R. Das[p], Zhongnan Dong[h,t,a], Luis Galbany[w,x], Noa Grollimund[p], Daniel Kelson[s], Dong Lai[y,z], Xia Li[h,i], Yuan Liu[a], Alessio Marino[w,x], Brenna Mockler[s], Paul O'Brien[aa], Erlin Qiao[a,f], Nanda Rea[w,x], L. Resmi[q], Jérome Rodriguez[p], Richard Saxton[ab], Luming Sun[g], Lian Tao[m], Tinggui Wang[j], Yilong Wang[a,w,x], Xuefeng Wu[ac], Dong Xu[a], Yijia Zhang[ad], Guoying Zhao[h], Congying Bao[a], Zhiming Cai[ae], Yehai Chen[ae], Yong Chen[n], Bertrand Cordier[af], Chenzhou Cui[a], Weiwei Cui[n], Zhou Fan[a,f], He Gao[l,ag], Giancarlo Ghirlanda[r,ah], Ju Guan[n], Dawei Han[n], Jinxin Hao[a], Jingwei Hu[a], Maohai Huang[a], Yong-Feng Huang[ai,aj], Shumei Jia[n], Ge Jin[ak], Stefanie Komossa[al], Chengkui Li[n], Zhixing Ling[a,f,l], Congzhan Liu[n], Heyang Liu[a], Huaqiu Liu[ae], Fangjun Lu[n], Kirpal Nandra[am], Jan-Uwe Ness[an], Arne Rau[am], Jeremy Sanders[am], Liming Song[n], Roberto Soria[ao,ap], Shengli Sun[aq], Xiaojin Sun[aq], Yuyin Tan[ar], Eleonora Troja[m], Sixiang Wen[a], Haitao Xu[ar], Changbin Xue[ar], Yongquan Xue[j], Yi-Han Iris Yin[c,d], Chen Zhang[a,*], Shuang-Nan Zhang[n], Yonghe Zhang[ae]

[a] National Astronomical Observatories, Chinese Academy of Sciences, Beijing 100101, China
[b] Institute for Astrophysics, School of Physics, Zhengzhou University, Zhengzhou 450001, China
[c] The Hong Kong Institute for Astronomy and Astrophysics, The University of Hong Kong, Hong Kong 999077, China
[d] Department of Physics, The University of Hong Kong, Hong Kong 999077, China
[e] Shenzhen Institute of Research and Innovation, The University of Hong Kong, Shenzhen 518057, China
[f] School of Astronomy and Space Science, University of Chinese Academy of Sciences, Beijing 100049, China
[g] Department of Physics, Anhui Normal University, Wuhu 241002, China
[h] School of Physics and Astronomy, Sun Yat-sen University, Zhuhai 510982, China
[i] CSST Science Center for the Guangdong-Hong Kong-Macao Greater Bay Area, Zhuhai 519082, China
[j] Department of Astronomy, University of Science and Technology of China, Hefei 230026, China
[k] Department of Astronomy, School of Physics, Huazhong University of Science and Technology, Wuhan 430074, China
[l] Institute for Frontier in Astronomy and Astrophysics, Beijing Normal University, Beijing 102206, China
[m] Department of Physics, University of Rome "Tor Vergata", via della Ricerca Scientifica 1, Rome I-00133, Italy
[n] Key Laboratory of Particle Astrophysics, Institute of High Energy Physics, Chinese Academy of Sciences, Beijing 100049, China
[o] Polar Research Institute of China, Shanghai 200136, China
[p] Université Paris Cité, Université Paris-Saclay, CEA, CNRS, AIM, Gif-sur-Yvette F-91191, France
[q] Indian Institute of Space Science and Technology, Trivandrum 695547, India
[r] INAF–Osservatorio Astronomico di Brera, Via Bianchi 46, I-23807 Merate (LC) I-23807, Italy
[s] The Observatories of the Carnegie Institution for Science, Pasadena, CA 91101, USA
[t] Université Paris Cité, CNRS, Astroparticule et Cosmologie, Paris F-75013, France
[u] Dipartimento di Fisica, Università di Napoli "Federico II", Compl. Univ. di Monte S. Angelo, Via Cinthia I-80126, Italy
[v] South-Western Institute for Astronomy Research, Yunnan University, Kunming 650504, China
[w] Institute of Space Sciences (ICE, CSIC), Campus UAB, Carrer de Can Magrans s/n, Barcelona E-08193, Spain
[x] Institut d'Estudis Espacials de Catalunya (IEEC), Barcelona E-08034, Spain
[y] Tsung-Dao Lee Institute, Shanghai Jiao Tong University, Shanghai 201210, China
[z] Center for Astrophysics and Planetary Science, Department of Astronomy, Cornell University, Ithaca, NY 14853, USA
[aa] School of Physics and Astronomy, University of Leicester, Leicester LE1 7RH, UK
[ab] Telespazio UK for ESA, ESAC, Apartado 78, Villanueva de la Cañada 28691, Spain

* Corresponding authors.
E-mail addresses: wdzhang@nao.cas.cn (W. Zhang), wmy@nao.cas.cn (W. Yuan), ccjin@nao.cas.cn (C. Jin), lixindai@hku.hk (L. Dai), chzhang@bao.ac.cn (C. Zhang).
[1] These authors contributed equally to this work.

https://doi.org/10.1016/j.scib.2025.12.050

[ac] Purple Mountain Observatory, Chinese Academy of Sciences, Nanjing 210023, China
[ad] Department of Astronomy, Tsinghua University, Beijing 100084, China
[ae] Key Laboratory for Satellite Digitalization Technology, Innovation Academy for Microsatellite, Chinese Academy of Sciences, Shanghai 201304, China
[af] CEA Paris-Saclay, Irfu/D'epartement d'Astrophysique, Gif sur Yvette 9111, France
[ag] School of Physics and Astronomy, Beijing Normal University, Beijing 100875, China
[ah] INFN–Sezione di Milano-Bicocca, Piazza della Scienza 3, Milano, MI I-20146, Italy
[ai] School of Astronomy and Space Science, Nanjing University, Nanjing 210023, China
[aj] Key Laboratory of Modern Astronomy and Astrophysics (Nanjing University), Ministry of Education, Nanjing 210023, China
[ak] North Night Vision Technology Co., LTD, Nanjing 210008, China
[al] Max-Planck-Institut fuer Radioastronomie, Auf dem Huegel 69, Bonn 53121, Germany
[am] Max-Planck-Institut für extraterrestrische Physik, Giessenbachstrasse 1, Garching 85748, Germany
[an] European Space Agency, European Space Astronomy Centre, Madrid E-28692, Spain
[ao] INAF-Osservatorio Astrofisico di Torino, Pino Torinese I-10025, Italy
[ap] Sydney Institute for Astronomy, School of Physics A28, The University of Sydney, NSW 2006, Australia
[aq] The Shanghai Institute of Technical Physics of the Chinese Academy of Sciences, Shanghai 200083, China
[ar] National Space Science Center, Chinese Academy of Sciences, Beijing 100190, China

A R T I C L E I N F O

Article history:
Received 19 October 2025
Received in revised form 2 December 2025
Accepted 12 December 2025
Available online 8 January 2026

Keywords:
X-ray transient
Intermediate-mass black hole
Tidal disruption event
White dwarf
Tianguan Einstein Probe

A B S T R A C T

Stars getting close enough to black holes (BHs) can be torn apart by strong tidal forces, producing electromagnetic flares. To date, more than 100 tidal disruption events (TDEs) have been observed, each involving invariably normal gaseous stars whose debris falls onto the BH, sustaining the flares over years. White dwarfs (WDs), which are the most prevalent compact stars and a million times denser–and therefore tougher–than gaseous stars, can only be disrupted by intermediate-mass black holes (IMBHs) of 10^2–10^5 solar masses. WD-TDEs are considered to generate more powerful and short-lived flares, but their evidence has been lacking. Here we report observations of a fast and luminous X-ray transient EP250702a detected by Einstein Probe. Its one-day-long X-ray peak as luminous as 10^{47-49} erg s^{-1} showed strong recurrent flares with hard spectra extending to several tens of MeV gamma-rays, as detected by *Fermi*/GBM and Konus-Wind, indicating relativistic jet emission. The jet's X-rays dropped sharply from 3×10^{49} erg s^{-1} to around 10^{44} erg s^{-1} within 20 days (10 days in the source rest frame). These characteristics are inconsistent with any previously known transient phenomena. We suggest that this fast-evolving event over the unprecedentedly short timescale arises likely from disruption of a WD by an IMBH. At late times, a soft component progressively dominates the X-ray spectrum, reaching a luminosity as high as 10^{44} erg s^{-1}, which is consistent with being extreme super-Eddington emission from an accretion disk expected to form in an IMBH-WD TDE. WD-TDEs open a new window for investigating the elusive IMBHs and their surrounding stellar environments, and they are prime sources of gravitational waves in the band of space-based interferometers.

1. Introduction

Intermediate-mass black holes (IMBHs), with masses in the range of 10^2–$10^5M_\odot$, occupying the mass gap between stellar-mass (a few to tens of solar masses) and supermassive black holes (SMBHs, with masses above $10^5M_\odot$), represent a critical missing link in the cosmic evolution of SMBHs [1,2]. Detections of IMBHs offer us great insights into the seeding and growth of SMBHs [3]. Tremendous efforts have been put on hunting IMBHs, especially in dwarf galaxies, globular clusters, and active nuclei of low-mass galaxies. However, very few candidates have been detected so far (e.g., Omega Centauri [4]).

When a star passes close enough to a black hole, it can be tidally disrupted and accreted, resulting in an electromagnetic outburst [5–7], which is known as tidal disruption events (TDEs). TDEs provide a unique probe for quiescent black holes which are otherwise difficult to detect, as well as an ideal laboratory for studying accretion around them. More than 100 TDEs have been discovered as X-ray, optical, and ultraviolet (UV) transients on timescales of months to years [8,9]. Tidal disruption events by IMBHs offer a novel approach to detect new IMBHs, to study their formation and evolution, and to investigate black hole accretion physics in this elusive mass regime [2].

It is particularly intriguing when the disrupted star is a white dwarf (WD) rather than a main sequence star, which is typically the focus of observation. WDs are the final evolutionary stage of most low- and intermediate-mass stars ($\lesssim 8M_\odot$). Compared with main sequence stars, WDs possess denser cores and stronger magnetic fields. Due to the compactness of WDs, they can only be disrupted by black holes with masses $\lesssim 10^5M_\odot$, making detections of WD-TDEs a smoking-gun evidence of IMBHs. It has been predicted that WD-IMBH TDEs will give rise to short-lived bright flares, potentially launch a relativistic jet, and may even be accompanied by a thermonuclear explosion triggered by the tidal compression of the WD [10,11]. However, no clear evidence for WD-IMBH TDE has been found hitherto, though this scenario was invoked to explain some of the observed properties in a few transients previously detected with short timescales (e.g., Refs. [12–14]).

In this paper, we report the discovery of a fast and luminous X-ray transient EP250702a by the Einstein Probe (EP[2]) [15] mission and follow-up observations and investigations. Its unique observed properties, including a long-duration X-ray and gamma-ray outburst, fast evolution of the transient X-ray light curve, an extremely high isotropic X-ray luminosity and rapid variability, the emergence of a soft component at a late stage of the X-ray spectral evolution, do

[2] The Einstein Probe is a space mission led by the Chinese Academy of Sciences (CAS), in collaboration with the European Space Agency (ESA), the Max Planck Institute for Extraterrestrial Physics (MPE) in Germany, and the French Space Agency (CNES).

not resemble those of any transients known previously. Instead, they all suggest the transient EP250702a to most likely arise from tidal disruption of a WD by an IMBH producing a relativistic jet.

Launched on 9 January 2024, EP is an interdisciplinary X-ray observatory with the main science goals being to detect cosmic X-ray transients. It carries 12 identical Wide-field X-ray Telescope (WXT) modules which utilize novel lobster-eye micro-pore optics (MPO) for X-ray focusing imaging. They achieve both a large instantaneous field of view (FoV; ~3850 square degrees) and relatively high sensitivity ($(2-3)\times10^{-11}$ erg s^{-1} cm^{-2} for 1 ks exposure), as well as good spatial resolution (~5′, full width at half maximum) across the entire FoV. These unique features make EP-WXT a powerful instrument for discovering X-ray transients and monitoring known sources. WXT's wide-field monitoring capability is complemented by an onboard Follow-up X-ray Telescope (FXT), with a FoV of 1°, for quick and deep follow-up observations.

2. Observations and data analysis

On 2 July 2025, the EP-WXT detected an X-ray transient exhibiting strong flaring activity, designated EP250702a [16]. The X-ray source was well localized with an uncertainty of only 2.4′ (90% C. L. statistical and systematic), thanks to the good spatial resolution of WXT. The source is spatially and temporally consistent with multiple gamma-ray flares, designated GRB 250702D, B, and E (hereafter GRB 250702B), each lasting several hundred seconds and together spanning a period of more than three hours, as detected by the Gamma-ray Burst Monitor (GBM) onboard the *Fermi* Gamma-ray Space Telescope, with spatial uncertainties of 7.8°–14.7° [17,18]. Associated hard X-ray and gamma-ray flaring activity from this source was also detected by the Monitor of All-sky X-ray Image (MAXI) [19], Konus-Wind [20], and the Space Variable Objects Monitor (SVOM) [21]. A backward search in the EP-WXT data revealed the emergence of its X-ray emission already since 01:40:26 Coordinated Universal Time (UTC) on 1 July 2025 (defined as the trigger time), which is about one day before the onset of the reported gamma-ray flares (Fig. 1a; Supplementary material, observations and data reduction). A targeted backward search in the *Fermi*/GBM data also uncovered an untriggered weak flare at 11:55:18 UTC on 1 July 2025, whose localization is broadly consistent with that of EP250702a (Fig. S1 online; Supplementary material, observations and data reduction).

The detections of EP250702a and the associated GRB 250702B have triggered extensive campaigns of multi-wavelength follow-up observations. Based on the promptly well determined WXT position, EP-FXT observed EP250702a in a quick follow-up on 3 July (approximately two days after the trigger) and further pinned down the source with an uncertainty of 10″ [23] (Fig. 1b), thereby facilitating subsequent multi-wavelength follow-ups. The most precise X-ray localization was provided by a 15-ks observation with the *Chandra* Advanced CCD Imaging Spectrometer (ACIS) on 18 July (PI: D.Y. Li), as shown in Fig. 1c. The coordinates of the X-ray source are right ascension (R.A.) = 18h58m45.56s and declination (Dec.) = −7°52′26.1″ (J2000), with a 1σ uncertainty of 0.79″ that includes both statistical and systematic errors. A decaying near-infrared (NIR) counterpart, with an extremely red color and located off the nucleus of an underlying galaxy, was identified in Very Large Telescope (VLT) observations starting from 3 July, and a radio counterpart was detected with MeerKAT observations starting on 4 July [22]. These positions are both consistent with the X-ray localization (Fig. 1d), pinning down the transient at the outskirt of an external galaxy. The redshift of EP250702a was determined to be $z = 1.036 \pm 0.004$ based on a JWST spectroscopic observation [24]. We performed high-cadence monitoring observations of EP250702a by EP-FXT until about 40 days after the trigger, when the source became no longer detectable.

By combining the WXT and FXT data, we obtain a densely sampled, complete X-ray light curve of EP250702a (Fig. 2a). The light curve shows an initial outburst phase lasting for ~ 1 day and followed by a rapid decay (the "afterglow" phase) with the flux declining by more than five orders of magnitude within 20 days (about 10 days in the source rest frame). Assuming isotropic emission, the outburst reached an apparent X-ray luminosity as high as several times 10^{47} erg s^{-1} at the first detection of EP250702a on 1 July. This hard non-thermal emission (see below) persisted relatively steadily for about 10 h, followed by several hours (a factor of $(1+z) \sim 2$ shorter in the source rest frame) of intense X-ray flaring activity with variability amplitudes exceeding one order of magnitude and reaching 3×10^{49} erg s^{-1} at peaks. Concurrently, three exceptionally bright and high-energy gamma-ray flares were detected. Prior to the start of the first-detection observation, the source position was not covered by WXT for 5 h. Stacking the data acquired earlier yields an upper limit of 3.5×10^{46} erg s^{-1}. Thus the initial rising phase from the onset of the event to the outburst state cannot be constrained.

The extremely high apparent isotropic luminosity of 10^{47-49} erg s^{-1}, the hard non-thermal spectrum from X-ray to gamma-ray, and the rapid variability of the flares (see below) indicate that the X-ray emission is highly beamed, originating from a transient relativistic jet. The emergence of the X-rays about one day before the gamma-ray flares, together with the exceptionally long gamma-ray flare durations (spanning about 2 h and possibly extending beyond 14 h, in the source rest frame, if the untriggered gamma-ray flare on 1 July was also associated with EP250702a), argues against gamma-ray burst (GRB) scenarios, even those involving ultra-long GRBs (Figs. 2a and 3a). The behavior of EP250702a neither fits any known Galactic transients. Instead, the extremely prolonged outburst with highly variable fluctuations/flares closely resembles the rare class of jetted TDEs, such as SW J1644 and AT2022cmc (over-plotted on Fig. 2a), except that they have even longer flare timescales. In such events, accretion of fallback stellar debris powers relativistic outflows, producing luminous and energetic non-thermal outbursts in the X-ray and gamma-ray bands.

The short variability timescale of the early outburst phase indicates an IMBH powering this event. The light curves during the flaring episodes observed by *Fermi*/GBM reveal a short minimum variability timescale of 1.5 s, corresponding to 0.74 s in the source rest frame (Table S5 online; Supplementary material, timing analysis). Such a brief timescale places an upper limit on the characteristic size of the source emitting region, $R_E < 2.2\times10^{10}$ cm, which implies an IMBH with a mass of $M_{BH} < 7.5\times10^4 M_\odot$ given that R_E cannot be smaller than the radius of the black hole event horizon for a Schwarzschild black hole. This is further supported by its off-nuclear position within its host galaxy. We thus suggest that EP250702a provides likely the clearest evidence for a jetted TDE produced by an IMBH.

The X-ray flux of this event began to decay much earlier, with a significantly faster decaying rate than all previously documented jetted TDEs (Fig. 2a). Furthermore, its decay timescale is also substantially shorter than those of the three previously reported IMBH-TDE candidates, which typically exhibit years-long decay profiles [26–29]. We also note that its X-ray luminosity at the peaks of the outburst is at least 1–2 orders of magnitude higher than those of all the known jetted TDEs. The short evolutionary timescale, together with the highest peak luminosity in X-ray, points to a WD, rather than a main-sequence star, as the disrupted

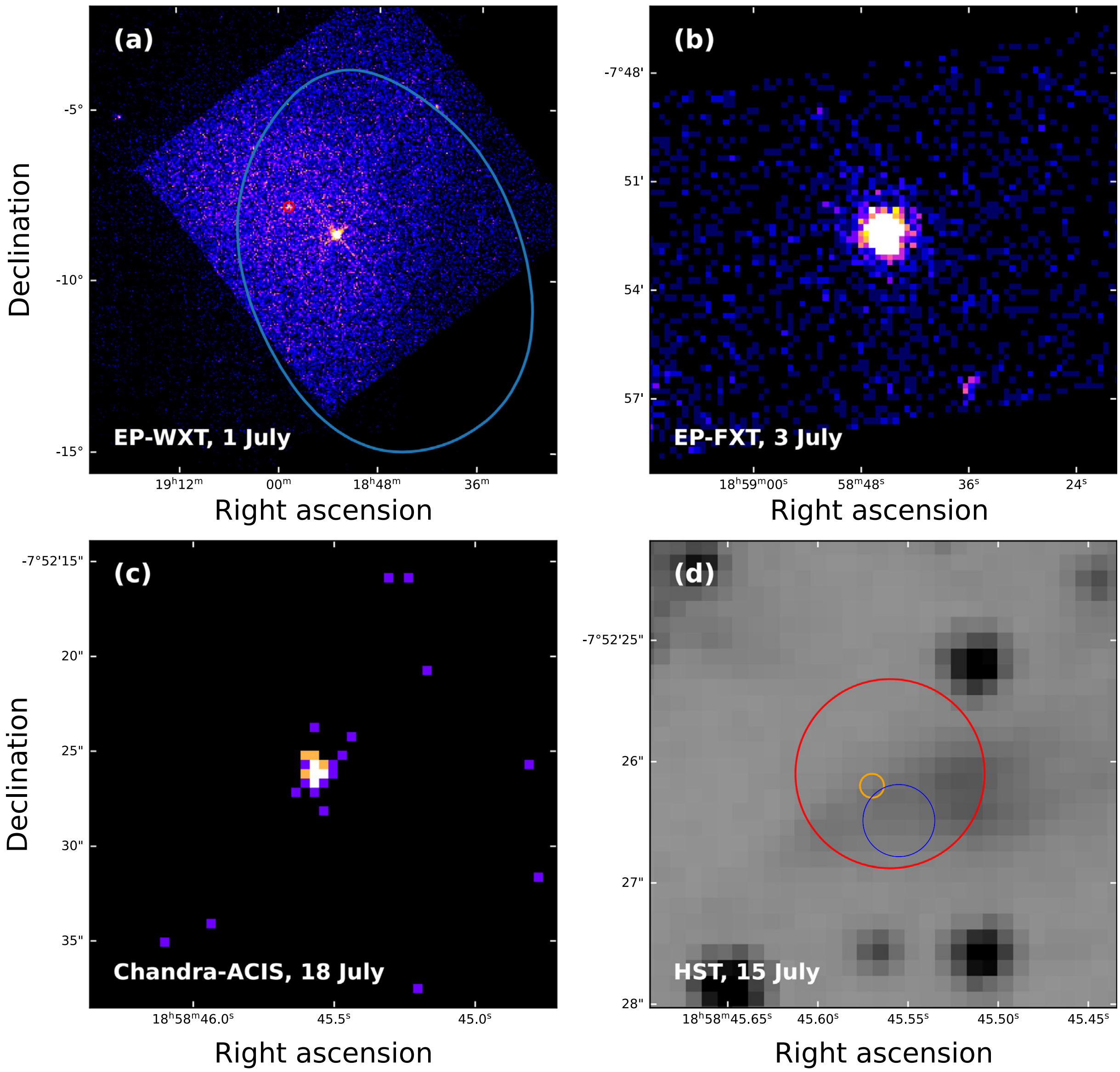

Fig. 1. The field of EP250702a in EP, *Chandra*, and HST imaging. (a–c) X-ray images of EP250702a taken by EP-WXT, EP-FXT, and *Chandra*, respectively. The position of EP250702a is indicated with red circles, and the blue contour shown in (a) gives the 1σ position uncertainty of GRB 250702B. (d) Optical image of EP250702a observed by HST. The red, orange, and blue ellipses indicate the positions of the X-ray, near-infrared (NIR), and radio counterparts of EP250702a, respectively. The NIR position and its uncertainties are obtained from VLT observations [22]. The radio position and its uncertainties are obtained from MeerKAT observations (Supplementary material, observations and data reduction).

star, since the fallback timescale for the latter would be much longer (tens of days or even longer) [30]. Our first-order theoretical scaling analysis further confirms that the rapid decay timescale of EP250702a is consistent with the tidal disruption of a low-mass WD by an IMBH (Figs. S7 and S8 online; Supplementary material, theoretical modelling).

Compared with other jetted TDEs, EP250702a also stands out by producing high-energy flares extending from the X-ray to the gamma-ray regime of several tens of MeV. (Fig. 3a). We extracted the 0.5 keV–38 MeV broad-band spectra of EP250702a from the EP-WXT and *Fermi*/GBM data for the flaring episodes, and found that the spectra are best fit with a non-thermal spectral model, characterized by a low-energy photon spectral index of approximately -1, a peak energy reaching up to 2 MeV, and a high-energy power-law component extending to several tens of MeV (Fig. 3b; Supplementary material, spectral analysis). The total fluence during the flaring phase, inferred from spectral fitting, is $\gtrsim(1.7\pm0.1)\times10^{-4}$ erg cm^{-2}, corresponding to an isotropic-equivalent energy of $\gtrsim(5.0\pm0.3)\times10^{53}$ erg at a redshift of $z=1.036$. This unprecedented high-energy peak at the gamma-ray band significantly exceeds the soft and hard X-ray regime typically observed in known jetted TDEs [31]. Based on the absence of a cutoff feature in the broad-band spectra, above which the pair-production opacity may reach unity, together with the observed variability timescale, we are able to place a lower limit on the jet bulk Lorentz factor under the assumption of the internal shock model. This yields $\Gamma_{\rm j}\gtrsim56$ (Supplementary material, constraints on the jet bulk Lorentz factor), which is similar to the values reported for previous jetted TDEs [31–33].

The WD-IMBH TDE scenario offers a natural explanation for the gamma-ray emission of EP250702a that is unique among jetted TDEs. The radiation mechanisms responsible for the flaring X-ray and gamma-ray emission of jetted TDEs remain unclear. Possible models include synchrotron radiation [31,34], synchrotron self-

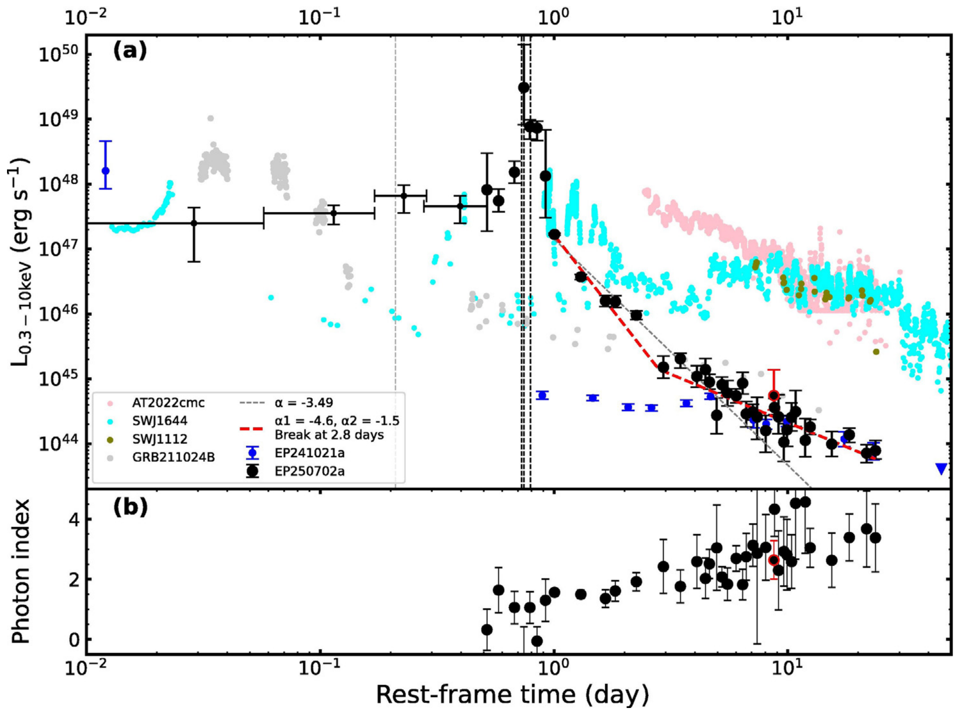

Fig. 2. Long-term X-ray light curve and spectral evolution of EP250702a. (a) Comparison of EP250702a with other X-ray transients, including jetted TDEs (Sw J1644+57, Swift J1112.2–8238, AT2022cmc), an ultra-long GRB (GRB 211024B) and a jetted TDE candidate EP241021a [25], on their X-ray light curves. The trigger time of EP250702a is set to be the start time of the first WXT observation when EP250702a begins to emerge (Supplementary material, observations and data reduction), about one day before the first *Fermi*/GBM trigger. The data points of EP250702a with red borders and red error bars represent measurement from the *Chandra* observation. The overlaid gray dashed line represents the single powerlaw decay fit, and the overlaid red dashed curve represents the two-segment power-law decay fit to the long-term X-ray light curve of EP250702a. The vertical dashed black lines denote the trigger times of the *Fermi*/GBM flares, and the vertical dashed gray one gives the time of the untriggered weak *Fermi*/GBM flare (Supplementary material, observations and data reduction). (b) The photon indices for EP250702a derived from absorbed power-law spectral fitting to the X-ray spectra. All error bars represent 1σ uncertainties.

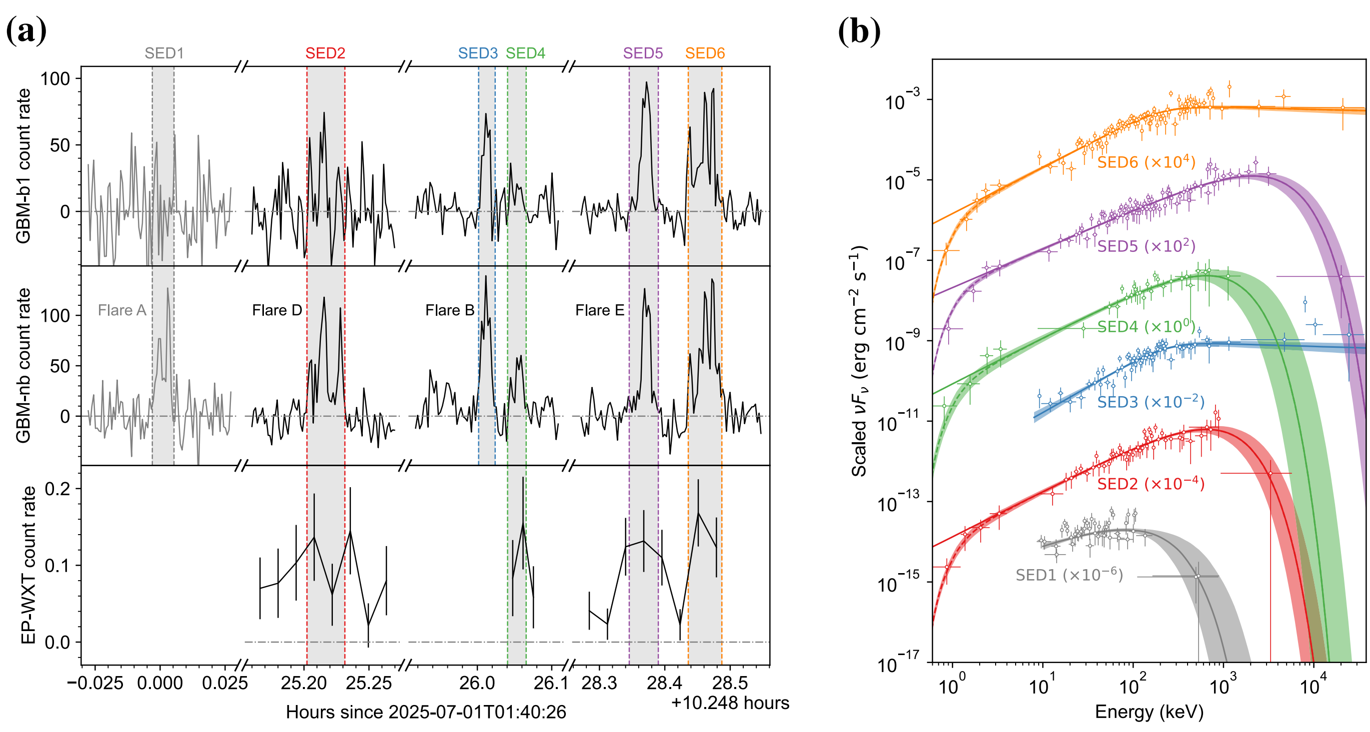

Fig. 3. Light curves and spectral energy distributions (SEDs) during the flaring episodes of EP250702a. (a) Light curves observed during the flaring episodes by the BGO detector of *Fermi*/GBM (top panel), the NaI detector of *Fermi*/GBM (middle panel), and EP-WXT (bottom panel). Six distinct flaring episodes are indicated by grey shaded regions with color-coded boundaries. (b) SEDs corresponding to the six flaring episodes. The SEDs are derived from the joint spectral fits over the time intervals indicated by the labels. Solid and dashed lines represent the best-fit unabsorbed and absorbed models, respectively. Error bars on the data points denote the 1σ confidence level, and the shaded regions around the best-fit lines indicate the corresponding 1σ confidence bands.

Compton (SSC [32,35]), and external inverse-Compton [32]. Although a larger Lorentz factor could lead to a higher peak energy, this is not the case for EP250702a as its Lorentz factor is comparable to other jetted TDEs. Another factor that determines the peak energy is the strength of the magnetic field if the radiation mechanism responsible for the high-energy emission is synchrotron or SSC. In this context, a magnetized WD as the disrupted star for EP250702a can offer a stronger magnetic field for the accretion disk that forms after the tidal disruption, thus pushing the peak energies to the gamma-ray band.

The extremely high X-ray luminosity at the first WXT detection of EP250702a indicates that the jet had already been launched by then. The initial flaring activity phase, with strong variabilities reaching peak luminosities two orders of magnitudes higher, lasted for almost one day. This implies that the process of launching and intensifying the jet in EP250702a takes longer compared with the typical debris fallback time scale expected for a WD-TDE by an IMBH. This may indicate that the disk formation and the magnetic flux accumulation processes [36], both needed for launching relativistic jets through the Blandford-Znajek process [37], likely happen over timescales much longer than the debris fallback timescale.

The flux decay is accompanied by dramatic spectral evolution, beginning with an extremely hard early-phase spectrum that progressively hardens during the period of flaring activity and then softens significantly during late-phase decay. This hard-to-soft transition is obvious by looking at the change of the photon index Γ of the spectrum that is measured by fitting an absorbed power-law model to the soft X-ray energy spectrum, which shows a clear transition from $\Gamma \approx 1$ to $\Gamma \approx 3$ (Fig. 2b), and evident by comparing X-ray spectra of early and late phases (Fig. 4a). Interestingly, the time from when the spectrum started to soften (several days after trigger) roughly coincides with a transition from steep ($f_X \propto t^{-4.6}$) to shallow ($f_X \propto t^{-1.5}$) decay in the X-ray flux evolution (Fig. 2a).

The spectral softening is accompanied by and probably is due to the emergence and gradual dominance of a thermal component during the late stage of the event. The break in the decay profile therefore indicates that the thermal component decays slower than the jet. The thermal component is significantly detected in the joint fit to the simultaneous *Chandra* and FXT observations taken about 17 days after trigger (Fig. 4b; Supplementary material, spectral analysis). The composite model combining blackbody that is used to describe the thermal component and the power-law, as demonstrated in Fig. 4b, yields a blackbody temperature of $kT = 169^{+37}_{-37}$ eV (typical of TDEs [38]), and a power-law index $\Gamma = 1.4^{+0.8}_{-0.8}$ that is consistent with the early-phase value. The unabsorbed flux of the thermal component is estimated to be 1.7×10^{-13} erg s^{-1} cm^{-2}, and the corresponding luminosity is 9.8×10^{44} erg s^{-1}.

The observed luminosity of the thermal component corresponds to $\sim 100 L_{\rm Edd}$ (the Eddington limit of a pure-hydrogen accretion disk) of a black hole of $7.5 \times 10^4 M_\odot$ in late time. While simulations of super-Eddington disks typically exhibit luminosities of $\lesssim 10 L_{\rm Edd}$ [39,40], WD-IMBH TDEs likely produce accretion disks with very high Eddington ratio and magnetization, which can lead to much higher disk luminosities [41]. Furthermore, this tension can be alleviated for a WD because, in the case of a fully ionized carbon–oxygen WD debris, the Eddington luminosity $L_{\rm Edd,CO}$ is twice $L_{\rm Edd}$ due to its lower electron scattering opacity. In the context of WD-IMBH TDEs, thermonuclear outbursts can occur, especially during deep tidal penetration events. As highlighted by MacLeod et al. (2016) [11], such outbursts are suggested to subtly affect the binding energy distribution of the debris, however their impact remains secondary to the gravitational dynamics that dom-

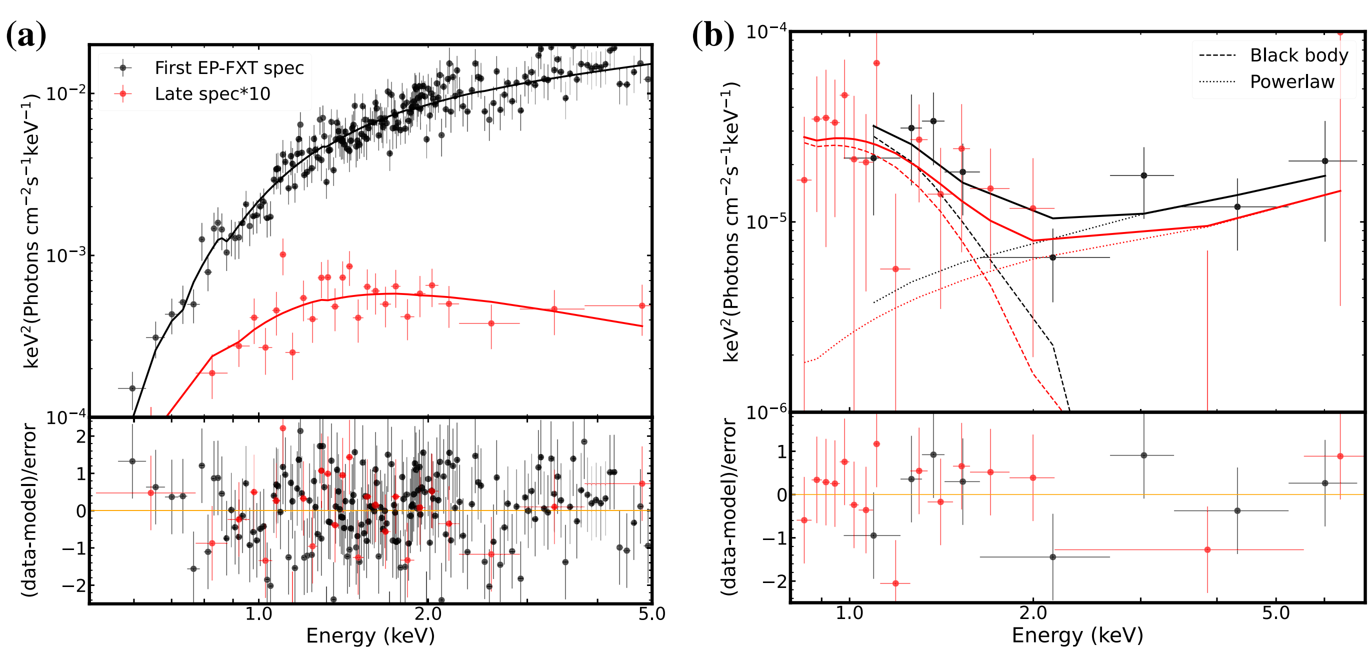

Fig. 4. X-ray spectra of EP250702a detected by EP and *Chandra*. (a) Evolution of X-ray spectra for EP250702a showing significant spectral softening trend in later observations. The spectrum taken from the first FXT observation on 2 July is shown in black points, and the late-time stacked spectrum (with the data taken from 12 July to 15 July, when the averaged spectral photon index is greater than 2) is shown in red. The late-time stacked spectrum has been scaled by a factor of 10 for visual clarity. Both spectra were fitted with an absorbed power-law model, and the fitting residuals were shown in the lower panel. (b) Joint X-ray spectral fitting of simultaneous *Chandra* and FXT observations, taken on 18 July, with the best-fit absorbed blackbody (dashed line) and power-law (dotted line) model components, as well as their combined model *const*tbabs*ztbabs*(bbody + powerlaw)* (solid line) (Supplementary material, spectral analysis). The fitting residuals are shown in the lower panel. The black and red points represent the *Chandra* and FXT observations, respectively. All error bars represent 1σ uncertainties.

inate accretion. Additionally, the outbursts themselves generate optical emission with peak luminosities around 10^{42} erg s^{-1}, which is significantly lower than the observed X-ray luminosity of 10^{44} erg s^{-1}. The total luminosity from these thermonuclear events is estimated to be $\sim 10^{41}(M_{\rm BH}/10^3 M_\odot)$ erg s^{-1} [42], with only a small fraction emerging in the soft X-ray band. Given that this luminosity falls below the detection limit at the redshift of EP250702a, the thermonuclear component is unlikely to significantly influence the observed accretion-driven light curve.

3. Discussion and conclusion

EP250702a exhibits rapid variability during early phases (hundred-second timescales), while the X-ray spectra photon index evolution demonstrates hardening–softening behavior unparalleled in comparison samples. This distinct timing signature, soft X-ray emission beginning about one day before the first *Fermi*/GBM trigger, provides an exceptional case study for IMBH accretion dynamics. EP250702a represents the first jetted TDE exhibiting late-phase spectral softening, characterized by unprecedented rapid evolution (more than five orders of magnitudes flux decline in 10 days in the source rest frame) and emergent thermal components consistent with an IMBH tidally disrupting a WD while launching relativistic jets. By modelling the near-infrared and radio light curves within the first month of its evolution in the context of synchrotron afterglow emission from the interaction of jet with the ambient medium, we find an isotropic kinetic jet energy of $E_{\rm K,iso} \approx 4.1 \times 10^{53}$ erg (Fig. S6 online; Supplementary material, afterglow modelling), which is comparable to that of the previously reported jetted TDEs [43].

We have examined several alternative models to interpret the event EP250702a (Supplementary material, other possible scenarios), including micro-tidal disruption events (μTDEs) involving stellar-mass black holes [44] and scenarios wherein a stellar-mass black hole spirals into a helium-star envelope via unstable mass transfer or common-envelope evolution [45]. Although these hypotheses present compelling theoretical possibilities, they face challenges in accounting for the full suite of observational features, particularly the luminous non-thermal X-ray emission detected approximately one day prior to the gamma-ray flares, significant spectral softening, and the off-center location within the host galaxy. Given these observational constraints, the jetted WD-IMBH TDE offers a more self-consistent and natural explanation for the observed properties of EP250702a.

The successful launch of a relativistic jet with an initial Lorentz factor of $\gtrsim 56$ (Supplementary material, constraints on the jet bulk Lorentz factor), implies a high spin of the black hole residing in EP250702a [37,46]. The dimensionless black hole spin parameter a is estimated to be around 0.6 at a redshift of 1.036 (Fig. S5 online; Supplementary material, constraints on the black hole spin). Either the IMBH was born with a high spin, or the IMBH was born as a stellar-mass black hole and grew via coherent accretion, while a growth history with chaotic accretion is disfavored [47]. Based on the luminosity of EP250702a, we estimate the event rate density of similar events to be $\sim 10^{-13}$ Mpc^{-3} yr^{-1} (Supplementary material, event rate density), which is orders of magnitude lower than what is expected for normal IMBH-TDEs and SMBH jetted TDEs. This low rate finds a natural explanation in the jetted TDE scenario through relativistic beaming, which limits detection to only a small fraction of events directed toward us. Future observations of sources analogous to EP250702a can provide further insights into the formation and evolution of IMBHs, the launch of relativistic jets in extremely high accretion systems, as well as their surrounding stellar environments. Perhaps of greatest interest, WD-TDEs are prime sources of simultaneous electromagnetic and gravitational wave (GW) emission in the sensitivity regime of future GW interferometers, allowing for important cosmological applications[3].

Conflict of interest

The authors declare that they have no conflict of interest.

Acknowledgments

This work was based on the data obtained with Einstein Probe, a space mission supported by the Strategic Priority Program on Space Science of Chinese Academy of Sciences, in collaboration with the European Space Agency, the Max-Planck-Institute for extraterrestrial Physics (Germany), and the Centre National d'Études Spatiales (France). This work was supported by the National Key Research and Development Program of China (2025YFF0511100), the National Natural Science Foundation of China (12333005, 12333004, and 12573019), and the Strategic Priority Research Program of the Chinese Academy of Sciences (XDB0550200). Jun Yang acknowledges the support from the National Natural Science Foundation of China (123B2044). Jin–Hong Chen and Lixin Dai acknowledge the support from the National Natural Science Foundation of China and the Hong Kong Research Grants Council (N_HKU782/23, HKU17314822, and HKU17305523). Chichuan Jin acknowledges the support from the National Natural Science Foundation of China (12473016, L2324211). Hui Sun acknowledges the support from the Young Elite Scientists Sponsorship Program by China Association for Science and Technology (YESS20240218). Jin–Hong Chen acknowledges the support from the National Natural Science Foundation of China (12503053). Weihua Lei acknowledges the support from the National Natural Science Foundation of China (12473012, 12533005). Yu-Han Yang acknowledges the support from the European Research Council through the Consolidator grant BHianca (101002761). Yongquan Xue acknowledges the support from the National Natural Science Foundation of China (12025303). Yong-Feng Huang acknowledges the support from the National Natural Science Foundation of China (12233002), the National Key Research and Development Program of China (2021YFA0718500), and the Xinjiang Tianchi Program. Sitha K. Jagan and L. Resmi acknowledge the support from the Anusandhan National Research Foundation (CRG/2002/008253). Sitha K. Jagan and L. Resmi thank Arvind Balasubramanian for useful discussions during the GMRT data analysis. We thank the staff of the GMRT for making these observations possible. This work was also based on observations made with the Gran Telescopio Canarias (GTC), installed at the Spanish Observatorio del Roque de los Muchachos of the Instituto de Astrofísica de Canarias, on the island of La Palma (GTCMULTIPLE2G-25A; PI: Francesco Coti Zelati). Francesco Coti Zelati is supported by a Ramøn y Cajal fellowship (RYC2021-030888-I). Francesco Coti Zelati, Alessio Marino, Yilong Wang and Nanda Rea acknowledge support from the Spanish grant (ID2023-153099NA-I00) and the programme Unidad de Excelencia María de Maeztu (CEX2020-001058-M). GMRT is run by the National Centre for Radio Astrophysics of the Tata Institute of Fundamental Research. Eleonora Troja acknowledges the support from the European Research Council through the Consolidator grant BHianca (101002761). Stefanie Komossa acknowledges the support from the President's International Fellowship Initiative of the Chinese Academy of Sciences. We acknowledge the National

[3] LISA mission webpage,https://www.lisamission.org/

Astronomical Science Data Center of China (NADC) for their contributions to the development of the EP time domain astronomical information center platform, including the observation data management, AI based transient identification agent, which supported the data processing and analysis in this work.

Author contributions

Weimin Yuan has been leading the Einstein Probe project as Principal Investigator since the mission proposal stage. Chichuan Jin, Lixin Dai, Weimin Yuan, Bing Zhang, Dongyue Li, Wenda Zhang, and Huaqing Cheng initiated the study. Chichuan Jin, Lixin Dai, Bing Zhang, Dongyue Li, Wenda Zhang, and Weimin Yuan coordinated the scientific investigations of the event and led the subsequent discussions. Bing Zhang, Lixin Dai, Rong-Feng Shen, Xinwen Shu, Weimin Yuan, Bifang Liu, Hongyan Zhou, Dongyue Li, Wenda Zhang, and Jun Yang contributed to the theoretical investigation of the event. Dongyue Li and Huaqing Cheng processed and analyzed the EP-WXT data. Dongyue Li performed the EP-WXT data backward-stacking and trigger time identification. Dongyue Li processed and analyzed the EP-FXT data. Dongyue Li, Huaqing Cheng, Chichuan Jin, and Lixin Dai obtained the *Chandra* observation data. Dongyue Li reduced the *Chandra* observation data. Jun Yang processed and analyzed the *Fermi*/GBM data. Jun Yang performed *Fermi*/GBM data targeted backward search and positional verification. Huaqing Cheng, Wenjie Zhang, and Haiwu Pan performed the Fourier power spectral density and Lomb–Scargle periodogram analyses of the EP-FXT data. Jun Yang performed the background modelling and duration calculation of *Fermi*/GBM data. Yu-Han Yang and Jun Yang calculated the minimum variability timescale of *Fermi*/GBM data. Jun Yang and Wenda Zhang constrained the black hole mass based on the minimum variability timescale. Dongyue Li performed the soft X-ray spectral analysis of the EP-WXT, EP-FXT and *Chandra* data. Dongyue Li contributed to the jet and disk spectral modelling. Jun Yang performed the joint soft X-ray and gamma-ray spectral analysis. Jun Yang contributed to constraining on the jet bulk Lorentz factor. Weihua Lei and Chang Zhou contributed to constraining on the black hole spin. Ning Jiang and Jiazheng Zhu contributed to the analysis on the host-galaxy properties. Fan Xu and Xinwen Shu performed the afterglow modelling. Jin–Hong Chen and Rong-Feng Shen performed the theoretical modelling of IMBH-WD TDE. Hui Sun contributed to the estimation of the event-rate density. Zhongnan Dong, Chun Chen, Xia Li, and Rong-Feng Shen contributed to the near-infrared data taking with SYSU-80 cm. Francesco Coti Zelati, Luis Galbany, Maria Cristina Baglio, Alessio Marino, Yilong Wang, and Nanda Rea contributed to the data acquisition and analysis with GTC. Brenna Mockler, Christopher R. Burns, and Daniel Kelson contributed to the NIR data taking with Magellan. Stéphane Corbel, Alexis Coleiro, Noa Grollimund, Floriane Cangemi, Jérome Rodriguez, and Xinwen Shu contributed to the radio data taking with MeerKAT. Sitha K. Jagan, L. Resmi, and Sourya R. Das contributed to the radio data taking with GMRT. Huaqing Cheng, Yijia Zhang, Chang Zhou, Yehao Cheng, and Guoying Zhan are the transient advocates, and Zhixing Ling is the duty scientist on 3 July 2025 and contributed to the discovery and preliminary analysis of this event. Zhixing Ling, Chen Zhang, Xiaojin Sun, Shengli Sun, Yonghe Zhang, Zhiming Cai and Weimin Yuan contributed to the development of the WXT instrument. Chen Zhang, Zhixing Ling, Huaqing Cheng, and Yuan Liu contributed to the calibration of WXT data. Yuan Liu, Huaqing Cheng, Chichuan Jin, Wenda Zhang, Dongyue Li, Jingwei Hu, Heyang Liu, and Haiwu Pan contributed to the development of WXT data analysis software. Yong Chen and Shumei Jia contributed to the development of the FXT instrument and the development of FXT data analysis software. Dongyue Li, Wenda Zhang, Jun Yang, and Weimin Yuan drafted the manuscript with the help from all authors.

Appendix A. Supplementary material

Supplementary data to this article can be found online at https://doi.org/10.1016/j.scib.2025.12.050.

References

[1] Volonteri M. The formation and evolution of massive black holes. Science 2012;337:544.
[2] Greene JE, Strader J, Ho LC. Intermediate-mass black holes. Annu Rev Astron Astrophys 2020;58:257–312.
[3] Inayoshi K, Visbal E, Haiman Z. The assembly of the first massive black holes. Annu Rev Astron Astrophys 2020;58:27–97.
[4] Häberle M, Neumayer N, Seth A, et al. Fast-moving stars around an intermediate-mass black hole in ωCentauri. Nature 2024;631:285–8.
[5] Hills JG. Possible power source of Seyfert galaxies and QSOs. Nature 1975;254:295–8.
[6] Rees MJ. Tidal disruption of stars by black holes of 10 to the 6th-10 to the 8th solar masses in nearby galaxies. Nature 1988;333:523–8.
[7] Komossa S. Tidal disruption of stars by supermassive black holes: status of observations. J High Energy Astrophys 2015;7:148–57.
[8] Saxton R, Komossa S, Auchettl K, et al. Correction to: X-ray properties of TDEs. Space Sci Rev 2021;217:18.
[9] Tidal Gezari S, Events disruption. Annu Rev Astron Astrophys 2021;59:21–58.
[10] Maguire K, Eracleous M, Jonker PG, et al. Tidal disruptions of white dwarfs: theoretical models and observational prospects. Space Sci Rev 2020;216:39.
[11] MacLeod M, Guillochon J, Ramirez-Ruiz E, et al. Optical thermonuclear transients from tidal compression of white dwarfs as tracers of the low end of the massive black hole mass function. Astrophys J 2016;819:3.
[12] Clausen D, Eracleous M. Probing intermediate-mass black holes with optical emission lines from tidally disrupted white dwarfs. Astrophys J 2011;726:34.
[13] Jonker PG, Glennie A, Heida M, et al. Discovery of a new kind of explosive X-ray transient near M86. Astrophys J 2013;779:14.
[14] Kuin NPM, Wu K, Oates S, et al. Swift spectra of AT2018cow: a white dwarf tidal disruption event? Mon Not R Astron Soc 2019;487:2505–21.
[15] Yuan W, Zhang C, Chen Y, et al. The einstein probe mission. arXiv: 2209.09763, 2022.
[16] Cheng HQ, Zhao GY, Zhou C, et al. EP250702a: an X-ray transient detected by Einstein Probe likely associated with GRB 250702B, C, D. E. GRB Coordinates Network 2025;40906:1. https://ui.adsabs.harvard.edu/abs/2025GCN.40906....1C/abstract.
[17] Neights E, Roberts OJ, Burns E, et al. *Fermi* GBM Triggers 250702B, C, D and E are likely from the same source. GRB Coordinates Network 2025;40891:1. https://ui.adsabs.harvard.edu/abs/2025GCN.40891....1N/abstract.
[18] Neights E, Roberts OJ, Burns E, et al. *Fermi* GBM analysis of GRB 250702B (formerly B, D, E); dissociation of C burst. GRB Coordinates Network 2025;40931:1. https://ui.adsabs.harvard.edu/abs/2025GCN.40931....1N/abstract.
[19] Kawakubo Y, Serino M, Negoro H, et al. MAXI/GSC detection of an X-ray activity from a transient associated with GRB 250702B, C, D, E and EP250702a. GRB Coordinates Network 2025;40910:1. https://ui.adsabs.harvard.edu/abs/2025GCN.40910....1K/abstract.
[20] Frederiks D, Lysenko A, Ridnaia A, et al. GRBs 250702B, C, D, E/ EP250702a: Konus-Wind detection of a hard X-ray transient activity. GRB Coordinates Network 2025;40914:1. https://ui.adsabs.harvard.edu/abs/2025GCN.40914....1F/abstract.
[21] Svom/Grm Team, Wang CW, Zheng SJ, et al. GRBs 250702B, C, D, E/ EP250702a: SVOM/GRM observation. GRB Coordinates Network 2025;40923:1. https://ui.adsabs.harvard.edu/abs/2025GCN.40923....1S/abstract.
[22] Levan AJ, Martin-Carrillo A, Laskar T, et al. The day-long, repeating GRB 250702BDE/EP250702a: a unique extragalactic transient. Astrophys J Lett 2025;990:14.
[23] Cheng HQ, Zhang YJ, Zhao GY, et al. EP250702a/GRB 250702B, C, D, E: EP-FXT follow-up observation. GRB Coordinates Network 2025;40917:1. https://ui.adsabs.harvard.edu/abs/2025GCN.40917....1C/abstract.
[24] Gompertz BP, Levan AJ, Laskar T, et al. JWST spectroscopy of GRB 250702b: an extremely rare and exceptionally energetic burst in a dusty, massive galaxy at z=1.036. arXiv: 2509.22778, 2025.
[25] Shu XW, Yang L, Yang HN, et al. EP241021a: a months-duration X-ray transient with luminous optical and radio emission. Astrophys J Lett 2025;990:L29.
[26] Lin D, Strader J, Carrasco ER, et al. A luminous X-ray outburst from an intermediate-mass black hole in an off-centre star cluster. Nat Astron 2018;2:656–61.
[27] Jin C C, Li D Y, Jiang N, et al. An intermediate-mass black hole lurking in a galactic halo caught alive during outburst. arXiv: 2501.09580, 2025.
[28] Yao Y, Chornock R, Ward C, et al. A massive black hole 0.8 kpc from the host nucleus revealed by the offset tidal disruption event AT2024tvd. Astrophys J Lett 2025;985:L48.

[29] He JS, Dou LM, Ai YL, et al. Long-term X-ray evolution of SDSS J134244.4 +053056.1. A more than 18 year-old, long-lived IMBH-TDE candidate. Astron Astrophys 2021;652:A15.

[30] Chen JH, Shen RF. Tidal disruption of a main-sequence star by an intermediate-mass black hole: a bright decade. Astrophys J 2018;867:20.

[31] Burrows DN, Kennea JA, Ghisellini G, et al. Relativistic jet activity from the tidal disruption of a star by a massive black hole. Nature 2011;476:421–4.

[32] Bloom JS, Giannios D, Metzger BD, et al. A possible relativistic jetted outburst from a massive black hole fed by a tidally disrupted star. Science 2011;333:203.

[33] Andreoni I, Coughlin MW, Perley DA, et al. A very luminous jet from the disruption of a star by a massive black hole. Nature 2022;612:430–4.

[34] Yao Y, Lu W, Harrison F, et al. The on-axis jetted tidal disruption event AT2022cmc: X-ray observations and broadband spectral modeling. Astrophys J 2024;965:39.

[35] Pasham DR, Lucchini M, Laskar T, et al. The birth of a relativistic jet following the disruption of a star by a cosmological black hole. Nat Astron 2023;7:88–104.

[36] Tchekhovskoy A, Metzger BD, Giannios D, et al. Swift J1644+57 gone MAD: the case for dynamically important magnetic flux threading the black hole in a jetted tidal disruption event. Mon Not R Astron Soc 2014;437:2744–60.

[37] Blandford RD, Znajek RL. Electromagnetic extraction of energy from Kerr black holes. Mon Not R Astron Soc 1977;179:433–56.

[38] Komossa S. Ludwig Biermann award lecture: X-ray evidence for supermassive black holes at the centers of nearby, non-active galaxies. Reviews in Modern Astronomy 2002;15:27.

[39] Sadowski A, Narayan R, McKinney J C, et al. Numerical simulations of super-critical black hole accretion flows in general relativity. Mon Not R Astron Soc 2014;439:503–520.

[40] Jiang YF, Stone JM, Davis SW. Super-Eddington accretion disks around supermassive black holes. Astrophys J 2019;880:67.

[41] McKinney JC, Dai L, Avara MJ. Efficiency of super-Eddington magnetically-arrested accretion. Mon Not R Astron Soc 2015;454:L6–L10.

[42] Rosswog S, Ramirez-Ruiz E, Hix WR. Tidal disruption and ignition of white dwarfs by moderately massive black holes. ApJ 2009;695:404–19.

[43] Zhou C, Zhu ZP, Lei WH, et al. AT2022cmc: a tidal disruption event with a two-component jet in a Bondi-profile circumnuclear medium. Astrophys J 2024;963:66.

[44] Beniamini P, Perets H B, Granot J. Ultra-long gamma-ray bursts from micro-tidal disruption events: the case of GRB 250702B. arXiv: 2509.22779, 2025.

[45] Neights E, Burns E, Fryer CL, et al. GRB 250702B: discovery of a gamma-ray burst from a black hole falling into a star. Mon Not R Astron Soc 2025;545:2.

[46] McKinney JC, Tchekhovskoy A, Blandford RD. General relativistic magnetohydrodynamic simulations of magnetically choked accretion flows around black holes. Mon Not R Astron Soc 2012;423:3083–117.

[47] Berti E, Volonteri M. Cosmological black hole spin evolution by mergers and accretion. Astrophys J 2008;684:822–8.